

**Supplementary data**

**Article title:** Time-to-event analysis of paclitaxel-associated peripheral neuropathy in advanced non-small cell lung cancer highlighting key influential treatment/patient factors

**Authors:** Francis W. Ojara, Andrea Henrich, Nicolas Frances, Wilhelm Huisinga, Niklas Hartung, Markus Joerger, Charlotte Kloft

**Journal title:** Journal of Pharmacology and Experimental Therapeutics

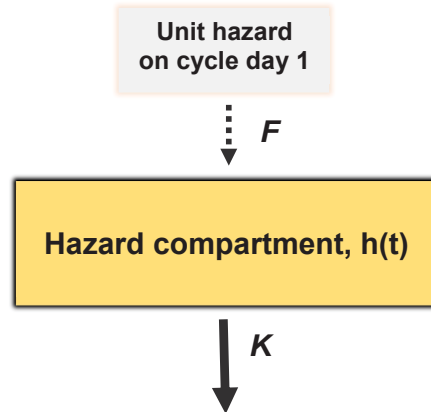
**Manuscript number:** JPET-AR-2020-000053

**Supplementary Table 1.** Parameter estimates (relative standard errors, %) for different hazard models analyzed to characterize the observed risk of 1<sup>st</sup> occurrence of PN2+

Parameter	Cycle-varying hazard	Constant	Weibull	Gompertz
OFV	1344.323	1368.727	1367.437	1367.321
$\lambda_0$ , day <sup>-1</sup>	-	0.00401 (9.60)	-	0.00342 (16.0)
$\lambda$ , day <sup>-1</sup>	-	-	0.00443 (12.4)	-
$\alpha$	-	-	1.10 (9.40)	-
$\beta$ , day <sup>-1</sup>	-	-	-	0.00323 (78.3)
$F$ , day <sup>-1</sup>	0.00568 (34)	-	-	-
$K$ , day <sup>-1</sup>	0.0560 (42)	-	-	-

$\lambda_0$ : Baseline hazard for the constant or Gompertz distributions;  $\lambda$ : hazard scale factor and  $\alpha$ : hazard shape factor for the Weibull distribution (unitless);  $\beta$ : exponential rate constant for the Gompertz distribution;  $F$ : hazard surge term for the cycle-varying hazard distribution;  $K$ : 1<sup>st</sup>-order hazard decay constant.

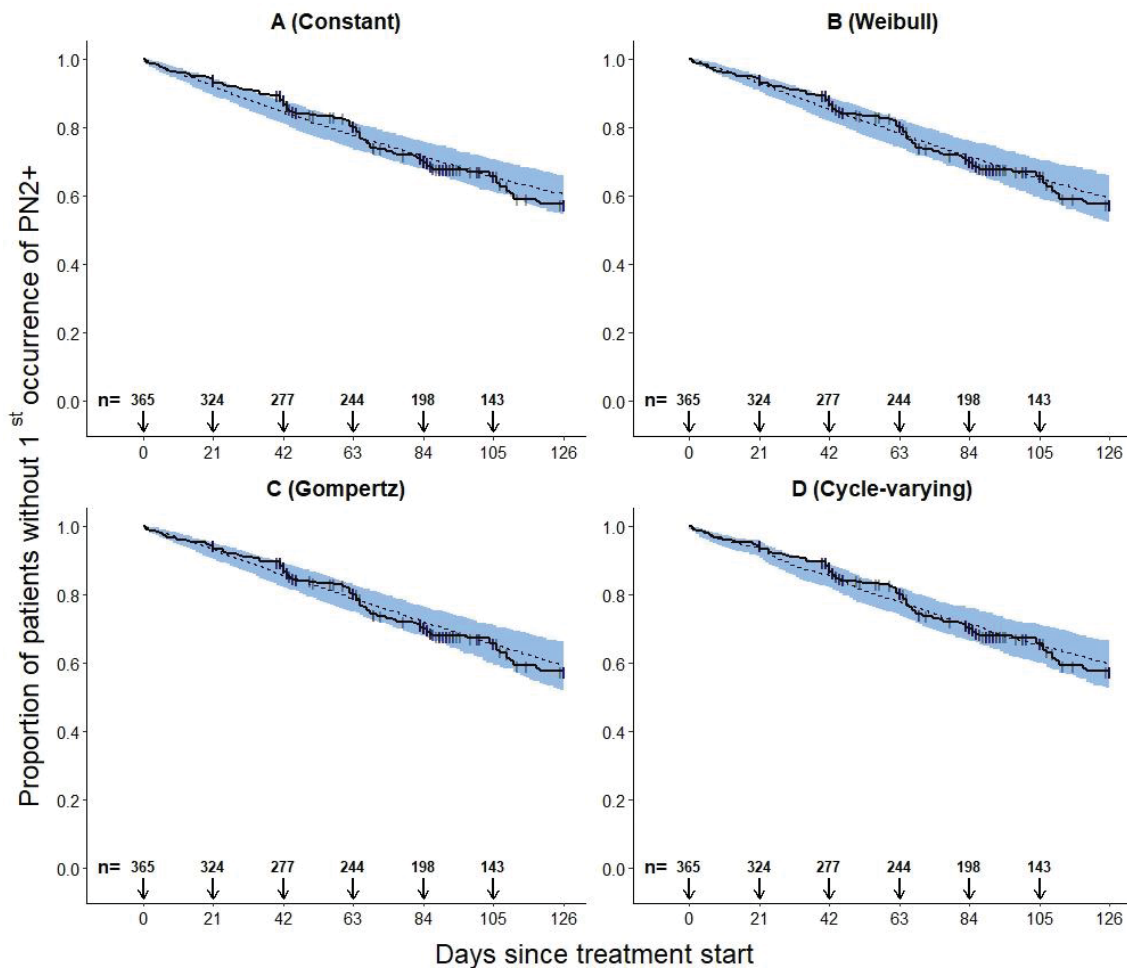
A schematic of the cycle-varying hazard model as implemented in the NONMEM software in this analysis



**Supplementary Figure 1.** Schematic of the cycle-varying hazard time-to-event model describing the hazard of 1<sup>st</sup> occurrence of peripheral neuropathy grades $\geq 2$  (PN2+) over time.  $F$ : hazard surge term;  $K$ : 1<sup>st</sup>-order hazard decay rate constant.

## **Evaluation of different TTE models**

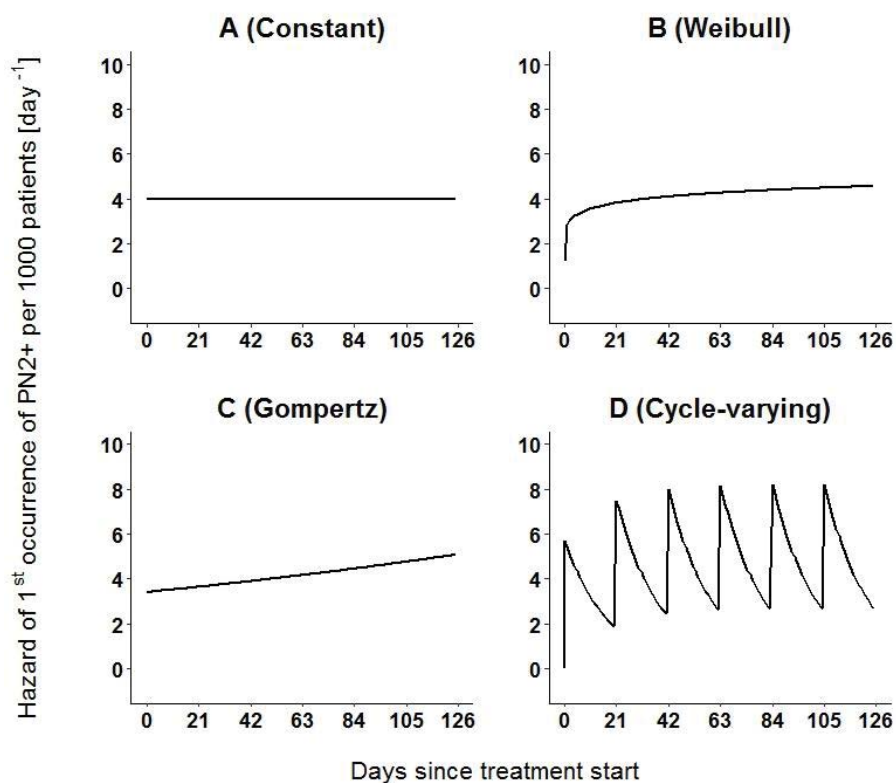
The visual predictive checks for the constant hazard, Weibull, Gompertz and cycle-varying hazard models is shown (Supplementary Figure 2). The median predicted profiles of the hazard of 1<sup>st</sup> occurrence of PN2+ across time was predicted by all the evaluated models. The cycle-varying hazard model, however, additionally described a cycle-specific trend showing a faster decline in proportion of patients without PN2+ at cycle start, followed by a more gradual decline across the cycle.



**Supplementary Figure 2:** Kaplan-Meier visual predictive checks comparing predictive performance of different hazard models to the observed peripheral neuropathy grades $\geq 2$  (PN2+) data. Proportion of patients without 1<sup>st</sup> occurrence of PN2+ across time on treatment is plotted with observations censored at the last protocol treatment day. Solid line: observed data (vertical lines represent censoring times), dashed line: median model predicted profile, with 90% confidence interval (blue shade); n: number of patients at specific observation times, corresponding to protocol treatment times.

## Predicted typical profiles of the hazard of 1<sup>st</sup> occurrence of PN2+ for different hazard models

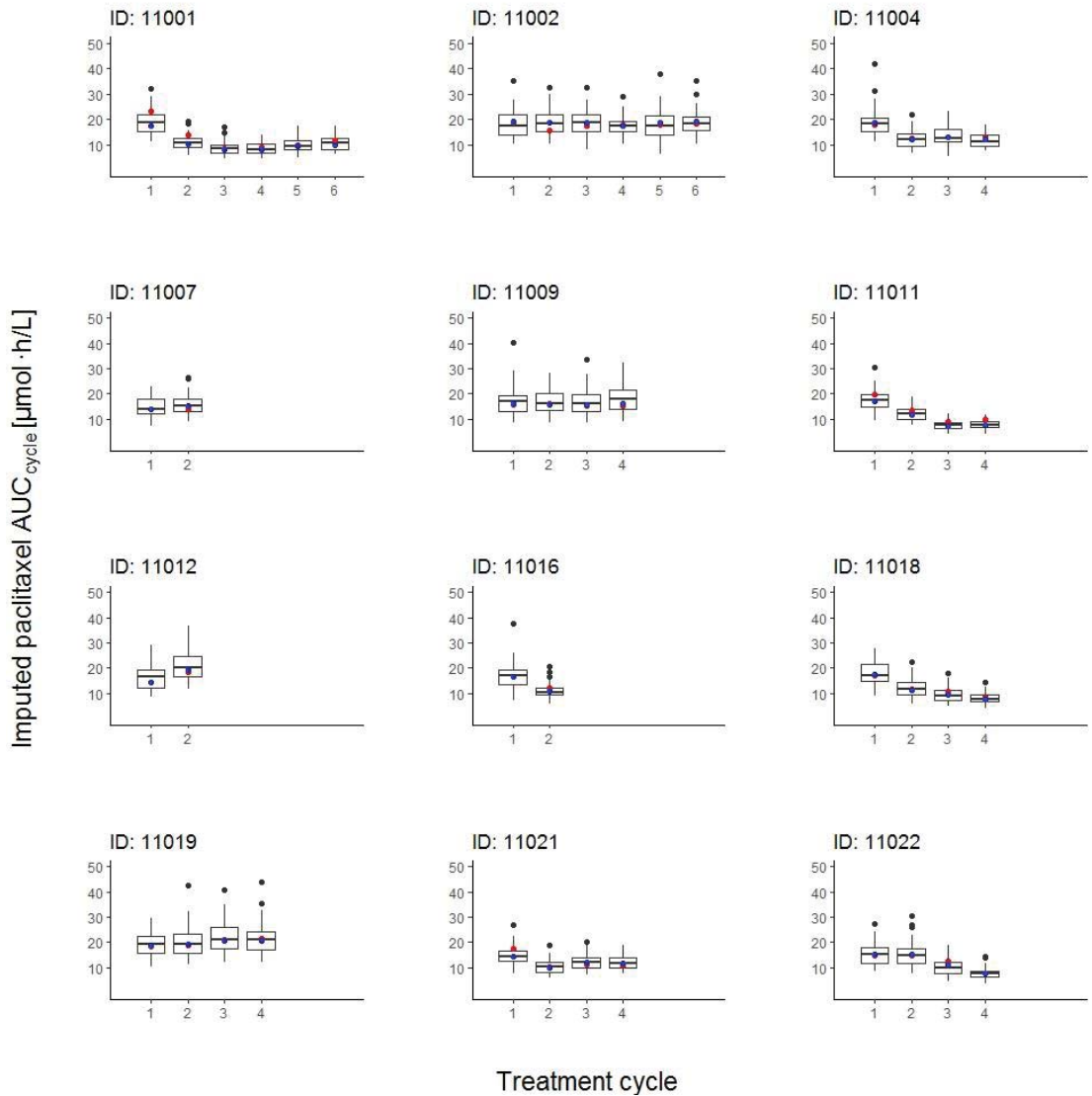
Profiles of hazard of 1<sup>st</sup> occurrence of PN2+ across time on treatment were generated by simulating the 1<sup>st</sup> occurrence of PN2+ for the 3-weekly paclitaxel dosing over 6 cycles using parameter estimates from different hazard models (Supplementary Table 1). The constant, Weibull and Gompertz hazard models described a monotonic change in hazard across time, whereas the cycle-varying hazard model described a surge in hazard at cycle start, and a subsequent gradual decline in hazard across the 21-day cycle, for all cycles (Supplementary Figure 3).



**Supplementary Figure 3.** Simulated typical profiles of the hazard of 1<sup>st</sup> occurrence of peripheral neuropathy grades  $\geq 2$  (PN2+) across time on treatment for different hazard models with standard paclitaxel dosing schedule. The hazard, scaled as risk of 1<sup>st</sup> occurrence of PN2+ for 1000 patients, was simulated for 3-weekly paclitaxel dosing over 6 cycles.

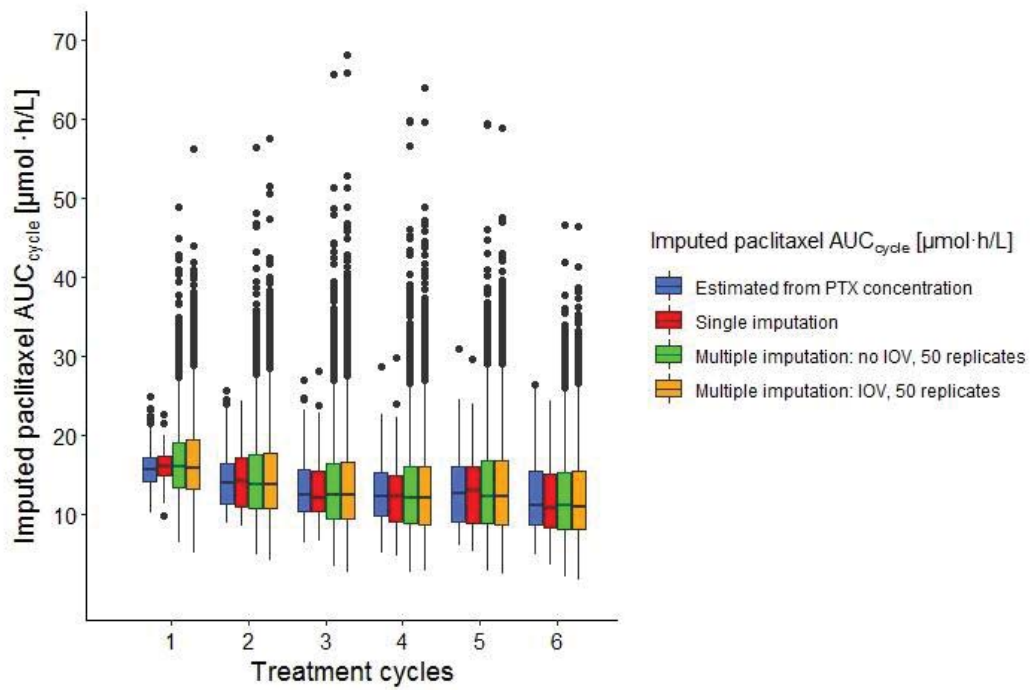
## **Imputation of paclitaxel PK and comparison of imputed and estimated paclitaxel exposure in the PK-guided dosing arm**

A paclitaxel PK model previously developed from data in the PK-guided dosing arm (Henrich et al., 2017) and individual patient characteristics were used to impute paclitaxel exposure (time of plasma concentrations above the thresholds 0.01  $\mu\text{M}$ , 0.05  $\mu\text{M}$ , and 0.1  $\mu\text{M}$  ( $T_{C>0.01\mu\text{M}}$ ,  $T_{C>0.05\mu\text{M}}$ , and  $T_{C>0.1\mu\text{M}}$ , respectively) and area under the plasma concentration-time curve between the start and end of a cycle ( $\text{AUC}_{\text{cycle}}$ ). For single imputation (SI), individual typical paclitaxel concentration-time profiles were predicted using the paclitaxel PK model and individual patient characteristics and different exposure metrics derived. For multiple imputation (MI), individual paclitaxel plasma concentration-time profiles (50 replicates) were predicted by stochastic simulations using the paclitaxel PK model and individual patient characteristics, and paclitaxel exposure metrics derived. Interoccasion variability in PK was accounted for with a treatment cycle considered an occasion. Paclitaxel  $\text{AUC}_{\text{cycle}}$  from SI closely matched the  $\text{AUC}_{\text{cycle}}$  estimated based on paclitaxel PK in the PK-guided dosing arm, and both fell largely within the interquartile range of paclitaxel  $\text{AUC}_{\text{cycle}}$  from MI, by comparison at both individual and population levels (Supplementary Figures 4, Supplementary Figures 5).



**Supplementary Figure 4:** Distribution of individual paclitaxel area under the plasma paclitaxel concentration-time curve between the start and end of a cycle ( $AUC_{cycle}$ ) across different cycles for selected representative patients in the PK-guided dosing arm. Boxes: interquartile range (IQR), including median of  $AUC_{cycle}$  from multiple imputation (MI); whiskers (vertical lines): range from box hinge, values within  $\pm 1.5 \cdot IQR$ ; red points: estimated paclitaxel  $AUC_{cycle}$  derived post-hoc from observed paclitaxel concentrations; blue points: paclitaxel  $AUC_{cycle}$  from single imputation; black points: simulated (MI) paclitaxel  $AUC_{cycle}$  using the paclitaxel PK model.



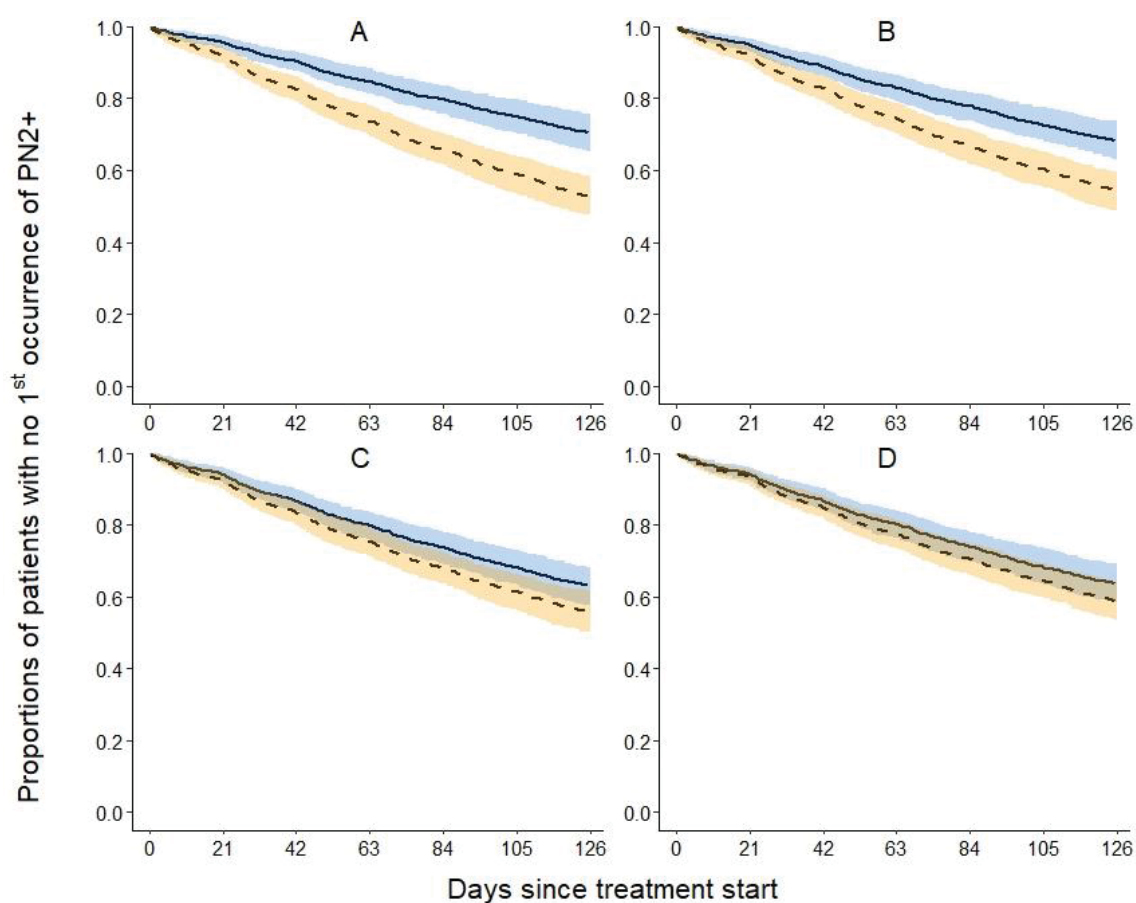


**Supplementary Figure 5:** Distribution of paclitaxel  $AUC_{cycle}$  across cycles in the PK-guided dosing arm.

Boxes: interquartile range (IQR), including median; whiskers (vertical lines): range from box hinge, values within  $\pm 1.5 \cdot IQR$ ; points: data beyond whiskers. IOV: interoccasion variability.

## Covariate impacts on the hazard of 1<sup>st</sup> occurrence of PN2+

Based on the FCM, clinical trials (n=250) were simulated at specific covariate levels based on the underlying distribution of the CEPAC-TDM dataset and Kaplan-Meier proportions of patients without 1<sup>st</sup> occurrence of PN2+ across time plotted. For the simulations, the 2.5<sup>th</sup> percentile of paclitaxel AUC<sub>cycle</sub> (7.32  $\mu\text{mol}\cdot\text{h/L}$ ), 2.5<sup>th</sup> percentile of age (47 years), females and current non-smokers were considered reference and evaluated against the 97.5<sup>th</sup> percentiles of paclitaxel AUC<sub>cycle</sub> (24.4  $\mu\text{mol}\cdot\text{h/L}$ ), 97.5<sup>th</sup> percentile of age (75 years), males and current smokers, respectively.

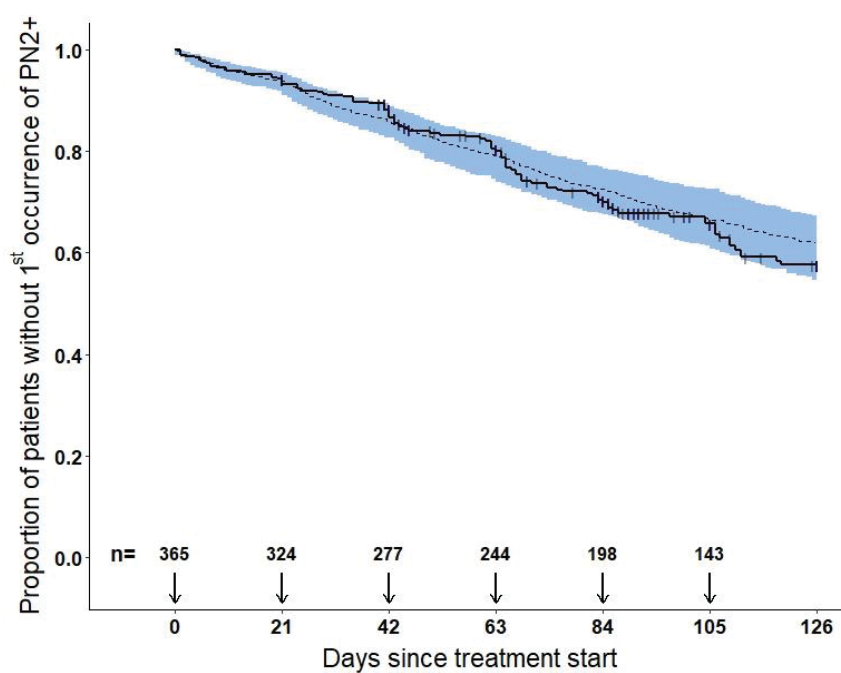


**Supplementary Figure 6:** Kaplan-Meier plots showing the risk of 1<sup>st</sup> occurrence of peripheral neuropathy grades $\geq$ 2 (PN2+) across time for different covariate levels based on the cycle-varying

hazard time-to-event full covariate model. Solid lines: reference covariate level, dashed lines: chosen covariate levels. Shades represent 90% confidence interval of proportions of patients experiencing 1<sup>st</sup> occurrence of PN2+, blue: reference covariate level, orange: chosen covariate. Panels: (A) paclitaxel  $AUC_{cycle}$  7.32  $\mu\text{mol}\cdot\text{h}/\text{L}$  (reference) versus 24.4  $\mu\text{mol}\cdot\text{h}/\text{L}$ , (B) age 47 years (reference) versus 75 years, (C) current non-smokers (reference) versus current smokers, (D) females (reference) versus males.

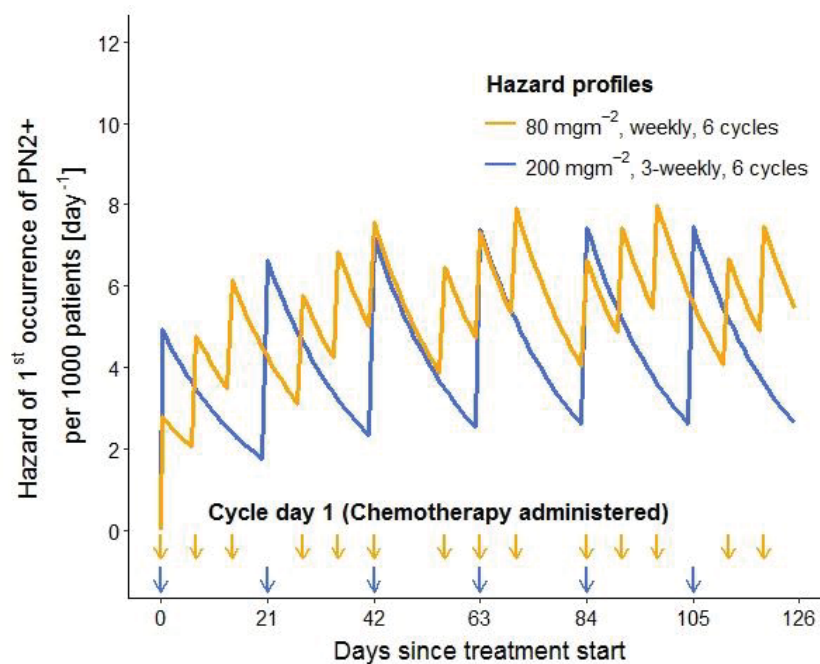
## Model evaluation of the cycle-varying hazard time-to-event FCM

Mean paclitaxel area under the plasma concentration-time curve between the start and end of each cycle ( $AUC_{\text{cycle}}$ ) were computed from individual imputed paclitaxel  $AUC_{\text{cycle}}$  (50 replicates) and used as input for each patient. 250 datasets were generated by simulation based on parameters derived from multiple imputations (Table 3), followed by graphical comparison of the simulated and observed data. Imputed parameter estimates adequately describe the observed data (Supplementary Figure 7).



**Supplementary Figure 7:** Kaplan-Meier visual predictive check for the cycle-varying hazard time-to-event full covariate model showing model prediction of 1<sup>st</sup> occurrence of peripheral neuropathy grades  $\geq 2$  (PN2+) based on multiple imputed model parameters. Proportion of patients without 1<sup>st</sup> occurrence of PN2+ is plotted across time with observations censored at the last protocol treatment time, solid line: observed data (vertical lines: censor times); dashed line: median model-predicted profile, 90% confidence interval (blue shade); n: number of patients at specific observation times; arrows: day of paclitaxel administration as specified in the study protocol.

## Typical profile of the hazard of 1<sup>st</sup> occurrence of PN2+ for two clinically-relevant paclitaxel dosing schedules



**Supplementary Figure 8:** Profiles of hazard of 1<sup>st</sup> occurrence of peripheral neuropathy grades  $\geq 2$  (PN2+) across time for two clinically-relevant paclitaxel dosing schedules in a typical patient (male, non-smoker of median age (64 years)). Orange arrows: dosing times for 80 mg/m<sup>2</sup> weekly dosing and blue arrows: dosing times for 200 mg/m<sup>2</sup> 3-weekly dosing. The end of the 6<sup>th</sup> cycles with 200 mg/m<sup>2</sup> 3-weekly dosing corresponds to 5 cycles of 80 mg/m<sup>2</sup> weekly dosing.